Parasitic Bipolar Junction Transistors in a Floating-Gate MOSFET for Fluorescence Detection

Kyeong-Sik Shin, Kyeong-Kap Paek, *Member, IEEE*, Jung-Ho Park, Tae-Song Kim, Byeong-Kwon Ju, and Ji Yoon Kang

***Abstract*—In this letter, we examined whether the parasitic bipolar junction transistors (BJTs) in the MOSFET fabricated by the standard CMOS process can play a role as a fluorescence detector. To suppress the action of two vertical parasitic BJTs, the gate and n-well were tied in the parasitic BJTs, and the body node was connected to the drain. The proposed device was compared with the inherent and the parasitic diodes in the MOSFET. It had 100 times higher photocurrents than the diodes in the MOSFET. In addition, it was applied for the detection of the fluorescent signal, and could detect near 10 nM of Alexa 546. Therefore, CMOS-process-compatible parasitic BJTs can be used as a photodetector in an integrated fluorescence detector.**

***Index Terms*—Biosensors, bipolar junction transistor (BJT), fluorescence, MOSFET, microfluidic, photodiode.**

I. Introduction

RECENTLY, many research groups have focused their work on highly integrated microfluidic systems. A significant challenge such as efficient detection of analyte molecules directly arises from the existence of small volumes within microfluidic systems. High-sensitivity detection is therefore a prerequisite for performing analysis in microfluidic systems [1], [2]. Some research groups reported that the p-i-n diode is used as a photodetector on silicon or glass substrates with laser system as an optical light source [3]–[5]. However, the p-i-n diode is not compatible with a CMOS fabrication process [6]. Matsumoto *et al.* and Matsunaga *et al.* proposed a new sensor using a counter-doped MOS transistor for its compatibility with the CMOS process [7], [8]. Although device structures have a lateral bipolar junction transistor (BJT) and two vertical parasitic BJTs, they did not consider the substrate (body) potential. Some groups including Zhang *et al.* reported that the enhancement-type floating-gate MOSFET on a silicon-on-insulator (SOI) substrate can play a role as a photodetector [9]–[11]. SOI MOSFETs have a buried oxide and then are absolutely isolated from the bulk silicon substrate. It means that they have no vertical parasitic BJT. Although these devices had a high gain property, their focus was concentrated on image sensing [12]. In general, as the fluorescent intensity becomes weaker, the fluorescence in the microfluidic system becomes harder to detect by using the p-n diodes in the CMOS process. Therefore, in this letter, we have designed the enhancement-type floating-gate MOSFET with two terminals using the standard CMOS process and examined the changes in the leakage current and gain with the body potential and the possibility that the device can be used as a photodetector (not integrated with a microfluidic channel) for the fluorescence detection in the microfluidic system.

Manuscript received March 14, 2007; revised May 2, 2007. This work was supported by the Intelligent Microsystem Center, which carries out one of the Twenty-First Century's Frontier R&D Projects sponsored by the Korea Ministry of Commerce, Industry and Energy and Korea Institute of Science and Technology grants. The review of this letter was arranged by Editor P. Yu.

K.-S. Shin, T.-S. Kim, and J. Y. Kang are with the Nano-Bio Research Center, Korea Institute of Science and Technology, Seoul 136-791, Korea (e-mail: jykang@kist.re.kr).

K.-K. Paek is with the Department of Electronic Engineering, Daejin University, Pocheon 487-711, Korea.

J.-H. Park and B.-K. Ju are with the School of Electrical Engineering, Korea University, Seoul 136-701, Korea.

Color versions of one or more of the figures in this letter are available online at http://ieeexplore.ieee.org.

Digital Object Identifier 10.1109/LED.2007.899999

II. Operation Mechanism and Fabrication Process

The structure of the proposed device reflecting the parasitic BJTs (p-BJTs) is shown in Fig. 1(a), which represents a schematic view of the parasitic p-n-p BJTs. The cross-sectional view of the BJT shows that the base of the p-BJT is formed by connecting the floating gate and the n-well with a single contact. When a positive voltage is applied to the drain and 0 V to the source, the potential of the drain channel decreased, and the electron–hole pairs (EHPs) can be made to flow in the channel region. In this bias condition, the potential barrier resembles the potential of a bipolar transistor in the forward bias condition and is used in the measurement procedure. When the external light was incident to the devices, the EHPs were generated in the interface of SiO_2/Si, which contributed to the base current in the p-BJT of MOSFET. Then, p-BJT amplified this base current (generated EHPs) into the drain current in the MOSFET. In this operational mechanism, the source, channel, and drain in the MOSFET corresponded to the emitter, base, and collector in p-BJT, respectively.

The devices were fabricated in the standard 1-poly, 2-metal, and n-well 1.5-μm CMOS process. As starting materials, p-type (100) silicon wafers with a resistivity of 10–20 $\Omega \cdot$ cm were used. The sheet resistances of drain and source were about 90 $\Omega/\square$. Aluminum is used as an electrode metal. The lateral diffusion length was about 0.2 μm.

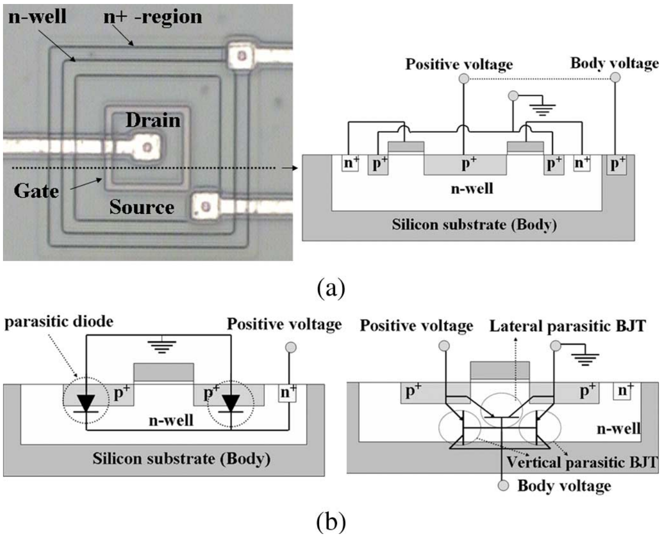

Fig. 1. Schematic of the devices fabricated and configuration of the bias condition: (a) Photograph and cross-sectional view of a floating gate MOSFET. (b) Operational mode: (left) a parasitic diode mode and (right) a parasitic BJT (p-BJT) mode in a floating-gate MOSFET under the bias condition.

III. Results and Discussion

The actual sizes of the designed devices were about 40 × 40 μm. Diode and floating-gate MOSFET photodetectors were formed into rectangular shapes on top of n-well, and each device was isolated by local oxidation of silicon (LOCOS). Fig. 1(a) shows the photograph of a floating-gate MOSFET. The diode has a shape identical to that of a MOSFET without the 1.5-μm polysilicon gate. A floating-gate MOSFET could be operated in two modes, namely, the parasitic diode and parasitic BJT (p-BJT) modes under the bias condition, as shown in Fig. 1(b). In the p-BJT mode, we noticed that two vertical p-BJTs exist in the drain–well–body and source–well–body regions. As EHPs are increased by the incident light into the device, the charges were accumulated in the lower well region, which lowered the barrier between the well and the body and then turned on the vertical p-BJTs in the body region. This phenomenon occurred repeatedly, and the current was oscillated with the variation of accumulated charges. Although, when the body was made to float, the drain current fluctuated, as shown in an inset box of Fig. 2(a). Fig. 2(a) shows the effect of body potential in the p-BJT with some incident light. When the body was connected to ground or some voltages, the drain current was at least 100 times higher than that when the body and the drain were tied due to the action of the vertical parasitic BJTs. Although the absolute current level was increased with the increasing difference of the drain and body voltages (V_{DB}), the light current to the dark current ratio was not significantly changed. The inset figure in Fig. 2(a) shows the body current as a function of the applied body–source voltage in a p-BJT. When the body voltage was negative value, the body current fluctuated in some points and reached -3.2 μA and 2 nA in the light and dark conditions, respectively. As the body voltage was close to the drain voltage, the fluctuation was reduced, and the body current decreased to 1.8 nA and 70 pA in the light and dark conditions, respectively. High body current is not desirable to isolate each device because it plays a role as a substrate leakage current. Especially, when V_{DB} was increased above 0.2 V, we noticed that the vertical p-BJTs can be turned on, as shown in Fig. 2(a). It implies that if the V_{DB} was maintained within 0.2 V, the body currents could be minimized without a significant reduction in the output current. It can be easily implemented to sustain the V_{DB} if the drain was connected to the body and the gate and n-well were tied in a floating-gate MOSFET.

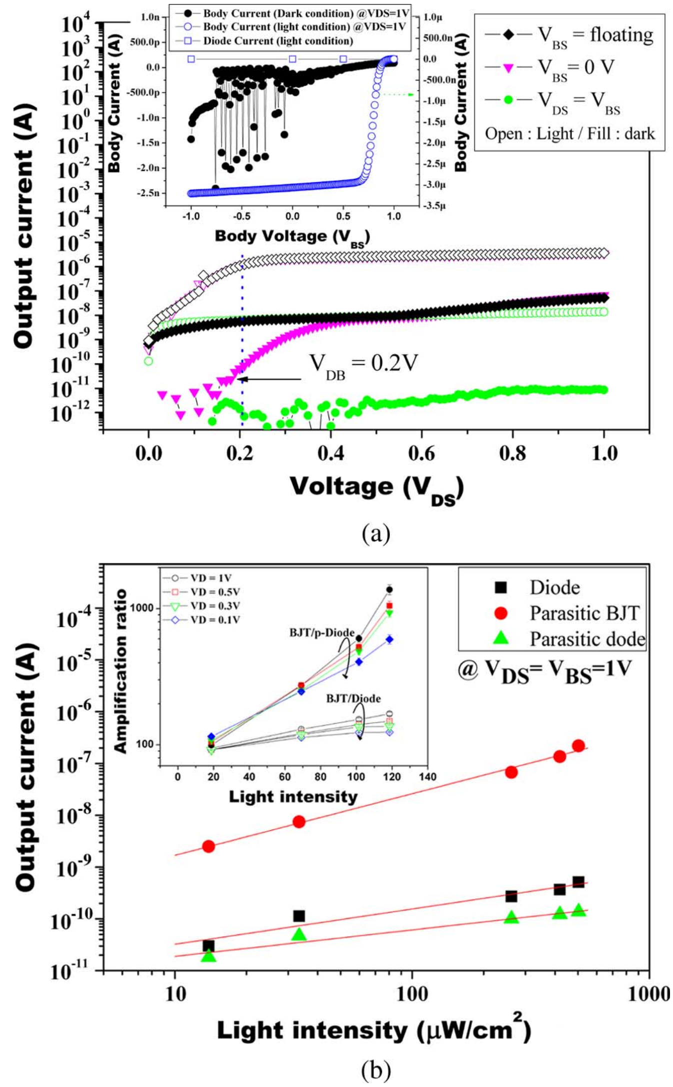

Fig. 2. Characteristics of a p-BJT. (a) Effect of body potential in the lateral p-BJT with some incident light; the inset box represents the body current as a function of the applied body–source voltage in the vertical p-BJTs. (b) Output current of p-BJT and diodes as a function of the light power of LED.

To compare optical characteristics of the p-BJT and the diode, we used a light-emitting diode (LED) as the only light power source in this experiment. Fig. 2(b) and the inset box represent the output current and amplification factor of the p-BJT and the diode as a function of the light power of LED, respectively. From the results, we observed that the current level of the p-BJT is at least 100 times higher than that of the diode and is comparable to that of the p-i-n diode due to the self-amplification effect of the p-BJTs [13]. Then, these

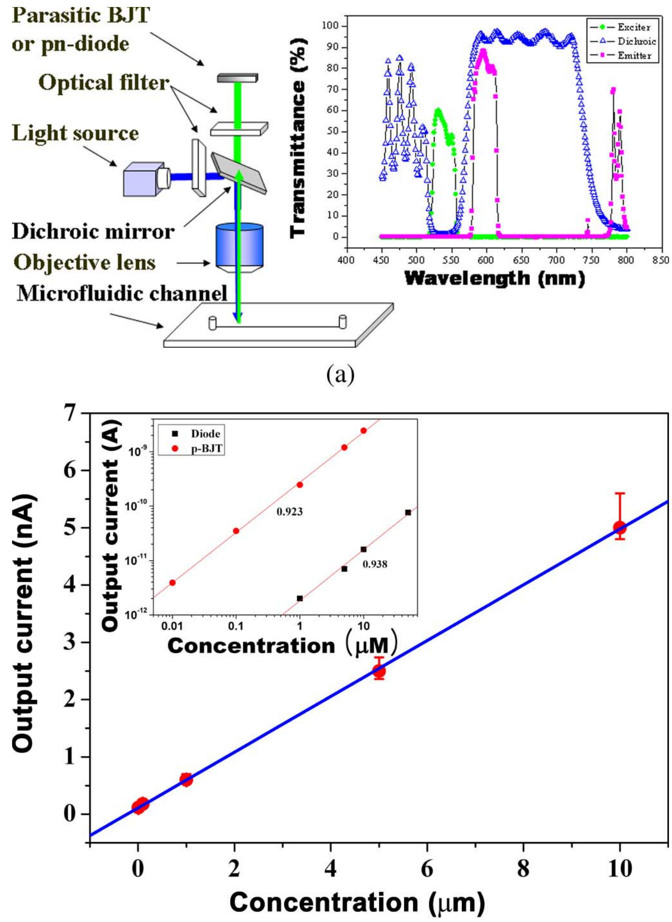

Fig. 3. Optical characteristics of the p-BJT and the diode. (a) Experimental setup. The inset box represents the characteristics of the optical filters (the flow rate is ∼1 mm/s, and the numerical aperture of the objective lens is ∼0.4). (b) Output currents of a p-BJT as a function of concentration with excitation light. The inset box represents the comparison of a p-BJT and a diode in florescence detection.

devices were applied to fluorescence detection as a photodetector component in the measurement system (Olympus BX51) in Fig. 3(a). The characteristics of the optical filters were shown in the inset box.

Alexa 546 is used as a fluorescent dye, which is excited and emitted at wavelengths of 555 and 570 nm, respectively. The polydimethylsiloxane microfluidic channel with dimensions of 100×30 μm was filled with Alexa 546. The fluorescent signal was monitored simultaneously by the p-BJT and the diode. Fig. 3(b) shows the output current of the p-BJT as a function of concentration. The background signal (BGS) is 42 pA, and the response slope is 0.243 nA/μM. To compare the p-BJT with the diode, the currents of the devices were plotted in the inset box. The figure shows the dependence of the BGS-subtracted fluorescent signal. A good linearity with fluorescence concentration is apparent (slope = 0.923, p-BJT and 0.938, diode) [14]. In the measurement, the p-BJT and diode can detect near 10 nM and above 1 μM of Alexa 546, respectively. However, there is a possibility that limit of detection (LOD) is getting worse when the detector is integrated to the microfluidic devices.

IV. Conclusion

We proposed the floating-gate MOSFET with two terminals, where the gate was tied with the n-well, and the body (substrate) was connected to the drain. The proposed device had 100 times higher photocurrents than the inherent or parasitic diodes in a MOSFET. Although its sensitivity was not higher than those in the previous reports [15], [16], it can be used as a photodetector in an integrated fluorescence detector because the LOD was dependent not only on the sensitivity of the photodetector but also on the optical methods (e.g., optical filter and optical path) in an integrated fluorescence detector. Therefore, we believe that the p-BJTs have a more significant advantage than the p-i-n photodiodes in an integrated fluorescence detector due to the merit of the integration with the additional electronic circuits using the CMOS process.

References

[1] K. B. Mogensen, H. Klank, and J. P. Kutter, “Recent developments in detection for microfluidic systems,” *Electrophoresis*, vol. 25, no. 21/22, pp. 3498–3512, Nov. 2004.

[2] A. M. Jorgensen, K. B. Mogensen, J. P. Kutter, and O. Geschke, “A biochemical microdevice with an integrated chemiluminescence detector,” *Sens. Actuators B, Chem.*, vol. 90, no. 1, pp. 15–21, Apr. 2003.

[3] M. E. Johnson and J. P. Landers, “Fundamentals and practice for ultrasensitive laser-induced fluorescence detection in microanalytical systems,” *Electrophoresis*, vol. 25, no. 21/22, pp. 3513–3527, Nov. 2004.

[4] M. L. Chabinyc, D. T. Chiu, J. C. McDonald, A. D. Stroock, J. F. Christian, A. M. Karger, and G. M. Whitesides, “An integrated fluorescence detection system in poly(dimethylsiloxane) for microfluidic applications,” *Anal. Chem.*, vol. 73, no. 18, pp. 4491–4498, Sep. 2001.

[5] K.-S. Shin, Y.-H. Kim, K.-K. Paek, J.-H. Park, E.-G. Yang, T.-S. Kim, J.-Y. Kang, and B.-K. Ju, “Characterization of an integrated fluorescence-detection hybrid device with photodiode and organic light-emitting diode,” *IEEE Electron Device Lett.*, vol. 27, no. 9, pp. 746–748, Sep. 2006.

[6] M. Kyomasu, “Development of an integrated high speed silicon PIN photodiode sensor,” *IEEE Trans. Electron Devices*, vol. 42, no. 6, pp. 1093–1099, Jun. 1995.

[7] K. Matsumoto, T. Nakamura, A. Yusa, and S. Nagai, “A new MOS phototransistor operating in a non-destructive readout mode,” *Jpn. J. Appl. Phys.*, vol. 24, no. 5, pp. L323–L325, May 1985.

[8] H. Yamamoto, K. Taniguchi, and C. Hamaguchi, “High-sensitivity SOI MOS photodetector with self-amplification,” *Jpn. J. Appl. Phys.*, vol. 35, no. 2B, pp. 1382–1386, Feb. 1996.

[9] S. A. Parke, C. Hu, and P. K. Ko, “Bipolar-FET hybrid-mode operation of quarter-micrometer SOI MOSFETs,” *IEEE Electron Device Lett.*, vol. 14, no. 5, pp. 234–236, May 1993.

[10] W. Zhang, M. Chan, S. K. H. Fung, and P. K. Ko, “Performance of a CMOS compatible lateral bipolar photodetector on SOI substrate,” *IEEE Electron Device Lett.*, vol. 19, no. 11, pp. 435–437, Nov. 1998.

[11] W. Zhang, M. Chan, and P. K. Ko, “Performance of the floating gate/body tied NMOSFET photodetector on SOI substrate,” *IEEE Trans. Electron Devices*, vol. 47, no. 7, pp. 1375–1384, Jul. 2000.

[12] Y. Matsunaga, H. Yamashita, S. Manabe, and N. Harada, “A high-sensitivity MOS photo-transistor for area image sensor,” *IEEE Trans. Electron Devices*, vol. 38, no. 5, pp. 1044–1047, May 1991.

[13] M. Krause, M. Topič, H. Stiebig, and H. Wagner, “Thin-film UV detectors based on hydrogenated amorphous silicon and its alloys,” *Phys. Stat. Sol.*, vol. 185, no. 1, pp. 121–127, May 2001.

[14] T. Kamei and T. Wada, “Contact-lens type of micromachined hydrogenated amorphous Si fluorescence detector coupled with microfluidic electrophoresis devices,” *Appl. Phys. Lett.*, vol. 89, no. 11, p. 114 101, Sep. 2006.

[15] T. Kamei, B. M. Paegel, J. R. Scherer, A. M. Skelley, R. A. Street, and R. A. Mathies, “Integrated hydrogenated amorphous Si photodiode detector for microfluidic bioanalytical devices,” *Anal. Chem.*, vol. 75, no. 20, pp. 5300–5305, Oct. 2003.

[16] J. R. Webster, M. A. Burns, D. T. Burke, and C. H. Mastrangelo, “Monolithic capillary electrophoresis device with integrated fluorescence detector,” *Anal. Chem.*, vol. 73, no. 7, pp. 1622–1626, Apr. 2001.